Article ID: 1006-8775(2003) 01-0031-10

ABRUPT CHANGES OF THE WESTERN PACIFIC SUBTROPICAL HIGH AND ITS INTERANNUAL VARIATION DURING LATE SPRING AND EARLY SUMMER

SHU Ting-fei (**舒廷飞**), LUO Hui-bang (**罗会邦**)

(1. *The Environmental Science and Engineering School, Zhongshan University, Guangzhou*, 510275 *China*)

ABSTRACT: The 500-hPa geopotential height data used in this paper are from NCEP/NCAR data set for the period from 1979 to 1996 (from March to July). Using pentad average, we define the intensity, westernmost ridge point and mean latitude of the subtropical high ridge. Then the wavelet transform and EOF analysis are performed. It is found that there mainly exist three interseasonal abrupt change processes, which correspond to the onset time of the South China Sea Summer Monsoon (SCSSM), the beginning and the end of the Mei-yu respectively. The interannual variation of the subtropical high in late spring and early summer presents quasi-4-year and 8-year periods.

Key words: West Pacific subtropical high; interannual variation; interseasonal mutation

CLC number: P447 **Document code:** A

1 INTRODUCTION

The subtropical high pressure is the most important circulation system in low latitudes. It is therefore one of the highly concerned subjects for meteorologists both at home and abroad to address the issue of the western Pacific subtropical high (to be simplified as WPSH), especially for summer. The study is roughly divided into three aspects[1]: The first one deals with the pattern with which the WPSH varies, which studies the shape, structure, nature and temporal / spatial changes etc.; the second one discusses a wide scope of factors governing the activity of the high; and the third one elaborates in the area of intraseasonal, intraannual, interannual and interdecadal variations of the WPSH and their relationship with the weather and climate. Among the work, the pattern with which the WPSH progresses and withdraws is the most studied and therefore the achievements on it are the most fruitful.

According to Huang Si-song, the characteristics and pattern concerning the change of the subtropical high can be of three kinds: seasonal, mid- and short- term and long-term[2]. Many attempts have been made with various types of data and methods and consistent, well-accepted conclusions have been drawn[1-6]. Most of the work, however, focuses on the variation of the WPSH over the summertime and pattern of seasonal migration, leaving little addressed with regard to the time from late spring to early summer. Using the latest and complete dataset of NCEP/NCAR for the 500-hPa geopotential field, the current work defines the intensity, the westernmost ridge point and ridge line that fit our own criteria and conducts a series of computation, wavelet transform and EOF analysis on them, in order to reveal its variation characteristics.

Received date: 2001–09–10; **revised date:** 2003–04–13

Foundation item: South China Sea monsoon experiment study —the Scaling Project A of the Ministry of Science and Technology of China; The first part of Key Foundamental Research Plan of China (G1998040900)

Biography: SHU Ting – fei (1974 –), male, native from Baise City of Guagnxi Zhuang Autonamous Region, Ph.D. candidate, undertaking the study of regional environmental study and synoptic dynamics.

2 DATA SOURCE, ARRANGEMENT AND INTRODUCTION TO DEFINITIONS AND ANALYSIS METHODS

2.1 *Data source and arrangement*

The work uses the NCEP/NCAR daily 500-hPa geopotential height field dataset for March – July from 1979 to 1996, which is 2.5°×2.5° in grid interval. The space selected is a domain bounded by 20°S – 40°N, 60°E – 180° and all of the data have been processed with pentad averaging.

2.2 *Definitions of the intensity, westernmost ridge point and ridge line of the WPSH*

For the definitions of the intensity, westernmost ridge point and ridge line of the WPSH, attempts have been made from various angles with generally consistent conclusions. As the main concern is about the characteristics of the subtropical high activity in late spring and early summer, the spatial coverage is selected and defined in a way somewhat different from previous work though with consistent basic ideas, adjusting to needs in question.

2.2.1 DEFINITION OF INTENSITY AND COVERAGE

Normally, the area index and center intensity are the characteristic indicators to show how powerful the WPSH is. The following definitions are used to describe the intensity of the high.

$$I = \sum_{j=1}^{N}\sum_{i=1}^{M}(H_{i,j} - 5880)\times d(H_{i,j} - 5880)$$

$$i=1, 2, \cdots\cdots, M; j=1, 2, \cdots\cdots, N$$

in which N and M are the sum of latitudinal and longitudinal gridpoints in the area of interest. $\delta(h)$ is the step function with the value taken as (0, 1) —1 is taken when $h \geq 0$; 0 is taken when $h<0$. $H_{i,j}$ represents all geopotential value at all gridpoints within the domain (10°N – 40°N, 80°E –180°).

2.2.2 DEFINITION OF WESTERNMOST RIDGE POINT

For the westernmost ridge point, it is defined here as the longitude of the contour 5880 at 500 hPa within the domain (10°N – 40°N, 80°E – 180°), with 2 or more of any eight adjoining gridpoints around the longitude being equal to or greater than 5880.

2.2.3 DEFINITION OF RIDGE LINE

For the ridge line, it is defined here as the latitudinal mean of all gridpoints enclosed by the contour 5890 in the 500-hPa geopotential height field within the domain (10°N – 40°N, 80°E –180°). The latitudinal mean of those encircled by the contour 5880 is used if the contour 5890 is not available. It can then be corrected by referring pentad-based variation of the corresponding 500-hPa geopotential height field.

2.3 *EOF analysis method*

Like all other orthogonal functions for decomposition, the EOF (Empirical Orthogonal Function) can be useful in this way.

Assuming that there is a meteorological field $F=f(T, X)$ in which t is the time and x is the serial number of spatial points. The values of meteorological elements for the j^{th} point at I^{th} time level are depicted $F_{mn} = \{f_{ij}\}(i = 1,2,\cdots, m;\ j = 1,2,\cdots, n)$. Specifically, m is the length of the time

series and n is the number of spatial gridpoints. The basic principle of the EOF is decomposing the meteorological field F into two parts that relate to time or space only. The part relating to space is composed of orthogonal functions, called eigenvectors; the part relating to time expresses the variation of individual orthogonal functions with time, called time coefficients. The whole process can be written as

$$F_{mn} = T_{mn} X_{nn}$$

here, F_{mn} is the original meteorological field, T_{mn} the matrix for the time coefficients and X_{nn} is a matrix made up of eigenvectors. With the method seeking matrix eigenvalues, the eigenvalues of $R=FF'$ is determined. Then, the eigenvectors and time coefficients for individual eigenvalues are sought. The methods are well known and will not be elaborated here.

The magnitude of an eigenvalue in the EOF decomposition represents an eigenvector it corresponds to, i.e. the weight of its canonical field and the time coefficient describes the variation of the field with time.

As shown in much research, a necessary condition for the EOF to stabilize is that meteorological data concerned have to be in steady time series and $m >> n$, which have been accounted for in the computation of the current work.

2.4 *Wavelet analysis*

The wavelet analysis is a mathematical approach recently developed, which differs from the Fourier analysis commonly used in two points: (1) the former method well reflects local temporal and spatial properties and (2) points to inter-links between different frequencies and reveals the changes in the magnitude of oscillations, which are different in the time scale and the extent of growth. The wavelet analysis has been applied widely in the atmospheric sciences since the 1990's. Much of the study has been documented and only those formula and information that are used in the work will be explained.

The Morlet wavelet is a plane wave that is modulated by the Gauss envelope of

$$y(t) = \mathrm{e}^{iw_0 t}\, \mathrm{e}^{-t^2/2}$$

with its Fourier transform being

$$w > 0$$

$$w \le 0$$

in which ω_0 is the wave vector, which usually takes ω_0=6.0.

In the text, the scale of stretch and shrink takes

$$a = 2^{(1+0.25(j-1))}$$

For the wavelet, the scale a is corresponding to each of the period T in the Fourier analysis

$$T = \frac{4pa}{w_0 + \sqrt{2 + w_0^2}}$$

For a given series to perform the wavelet transform, the modules of coefficients and contours distribution of the real parts are made. In the current work of wavelet transform, the ordinate on the left of the figures denotes the scale and the abscissa indicates the time in the unit of year. Its relationship with the ordinate is shown in Tab.1.

The coefficient module shows how periods of varying-time-scale distribute in the domain of time —the larger the module, the more obviously the corresponding time sections and scales are showing.

Tab.1 Relationship between the ordinate and its corresponding period in the wavelet analysis of interannual variation.

Ordinate	1	2	3	4	5	6	7	8	9	10	11	12	13
Corresponding period／yr.	2.0	2.4	2.8	3.4	4.0	4.8	5.7	6.7	8.0	9.5	11.3	13.5	16.0

3 ABRUPT CHANGE CHACTERISTICS OF WESTERN PACIFIC TROPICAL HIGH IN LATE SPRING AND EARLY SUMMER

3.1 *Pentad-based changes of multi-year averages of 500-hPa geopotential height field*

It is known from previous work that the 500-hPa geopotential height field of the subtropical high pressure is gradually intensifying and moving north as it goes from spring to summer and it experiences a process of eastward withdrawing and weakening around the onset of the South China Sea monsoon[13 - 18]. To study it in detail, we have conducted an averaging of the geopotential field data for Pentad 6 of April through Pentad 6 of May over the 18 years and plotted a figure (omitted) of pentad-to-pentad changes of the geopotential field and dynamic diagrams showing the temporal variation of the westernmost ridge point and subtropical high center (Fig.1 a & b). It is known from the multi-year mean of the field that the subtropical high is generally strengthening before Pentad 2 and after Pentad 4, of May. The principal part of the high, however, becomes smaller in size, the center travels north and east and the westernmost ridge point goes back from 108°E of Pentad 3 to around 117°E of Pentad 4, as shown in the multi-year mean of the 500-hPa geopotential height field. It directly links with the abrupt onset of the South China Sea monsoon in mid-May. In other words, there seems to be a well-defined abrupt change in the subtropical high, i.e. it weakens and withdraws towards the east, during the onset phase of the monsoon, as seen from the viewpoint of multi-year mean.

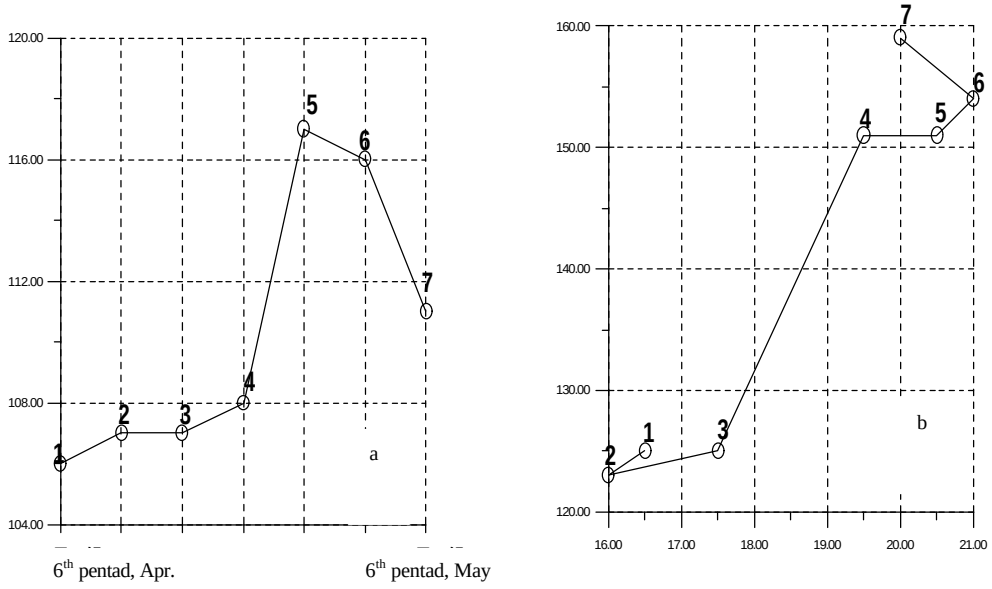

Fig.1 Temporal variation of the westernmost ridge point (a) and subtropical high center (b), with the ordinate being the longitude and the abscissa the pentad.

3.2 *Variations of the subtropical high intensity*

3.2.1 MEAN VARIATION TENDENCY OF SUBTROPICAL HIGH FOR MARCH – JULY OVER THE 18 YEARS

In terms of the intensity defined in previous text, we first seek a multi-year mean based on the 18-year pentad-to-pentad data, then obtain the mean for March – July and finally determine the deviations by subtracting the March – July mean from the multi-year mean for individual pentads. In this way, a figure showing multi-year mean evolution of the subtropical high intensity is made (Fig.2). It is a general reflection of general variation of the subtropical high intensity in March – July, which increases with time.

3.2.2 EOF ANALYSIS OF THE SUBTROPICAL HIGH INTENSITY

Conventionally, the EOF analysis is carried out of the time series of meteorological fields so that patterns with which some of the major spatial distribution of the fields are known with respect to time. First, the 18-year pentad-based March – July data of the subtropical high are processed with anomalous deviation and the yearly pentad-to-pentad intensity anomalies of the high intensity are used as a "spatial field". Its interannual variations are taken as the temporal variation part of the EOF analysis. The EOF analysis is then conducted. It reflects some of the major intraseasonal variations of the intensity and corresponding interannual variations during the period March through July.

Tab.2 gives the percentages of the first four eigenvectors in the EOF analysis of the subtropical high intensity and corresponding accumulative percentages. It is known from the table that the first eigenvector takes up about 40% of the total variance. It can generally represent the most pronounced characteristics of the intraseasonal variations.

Tab.2 Accumulative percentage of four basic eigenvectors and corresponding accumulative percentages for the intraseasonal variations of the subtropical high in late spring and early summer

Eigenvectors	first	second	third	fourth
Percentages / %	37.21	13.73	10.96	8.31
Accumulative percentages / %	37.21	50.94	61.90	70.21

Fig.3 depicts the first eigenvector of the intraseasonal variation of the subtropical high intensity, which tells about the predominant pattern. It shows a relatively smooth variation of the intensity before Pentad 3 of May, followed by a sudden weakening around Pentad 4 of May till the minimum point near Pentad 1 of June. It then increases rapidly and weakens once more around mid-June, reaching the lowest point in Pentad 1 of July before ascending again. In other words, the intensity has two obvious processes of weakening and strengthening in a reversed bimodal distribution. The first reduction in intensity happens between Pentad 3 and Pentad 5 in May, corresponding to the onset of the summer monsoon in the South China Sea; the first abrupt increase takes place between Pentad 2 and Pentad 3 in June, corresponding to the first northward jump of the subtropical high and the Mei-yu in the Changjiang R. Valley; the second intensification is seen between Pentad 3 and Pentad 5 in July, corresponding to the second northward jump of the subtropical high.

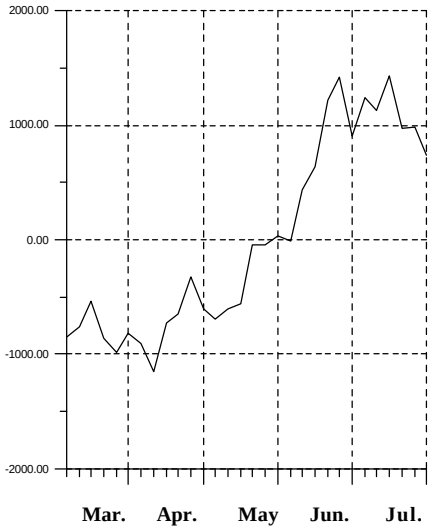

Fig.2 Deviation of pentad-to-pentad variation of 18-year mean evolution of the subtropical high intensity in March – July.

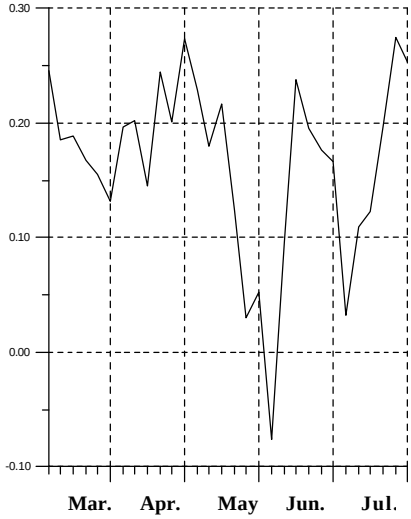

Fig.3 The first eigenvector of EOF analysis of the subtropical high intensity.

3.3 *Variation of the westernmost ridge point of the subtropical high*

3.3.1 MEAN VARIATION TENDENCY FOR MARCH THROUGH JULY OVER THE 18 YEARS

For the study of subtropical high activity patterns, more attention is placed on the north-south shift of the ridge line than on the variation of the westernmost ridge point, especially for the season from late spring to early summer. Much less work has been reported on the evolution of the westernmost point of the ridge. Tang et al[5]. used the data of 1954 – 1975 to determine its mean locations at 106°E, 114°E, 122°E, 124°E, 124°E, 118°E, and 117°E, respectively, which vary much from year to year. In this work, a more complete set of NCEP/NCAR data is used that covers the 500-hPa geopotential height field from March through July over the years 1979 – 1996. Following the definition about the westernmost ridge point set in the section above, we have identified its mean variations over the 18 years (Fig.4). It shows that the month-to-month mean is generally consistent with the result by Tang et al. and points to a significant abrupt change in Pentad 3 – Pentad 4 in May. It indicates that the westernmost ridge point can change dramatically, in other words, it suddenly withdraws to the east.

3.3.2 EOF ANALYSIS OF THE WESTERNMOST RIDGE POINT OF THE SUBTROPICAL HIGH

Like the intensity, we apply a similar processing of the westernmost ridge point. It is done by giving an anomalous treatment of the data about the point on the basis of pentad for March – July over the 18 years before the EOF analysis. It gives one the idea of several intraseasonal variations of the ridge point during the months and corresponding year-to-year changes.

As shown in the computation, the first eigenvector takes up about 25% of the total variance (table omitted). It can therefore represent the main features of the point's intraseasonal changes.

Fig.5 is the first eigenvector, which describes major intraseasonal variation patterns. It is shown in the figure that the point is quite unstable before mid-April but varies in a bimodal manner between mid-April and mid-July, in which three obvious east-west shifts are observed. The point begins the westward extension during the period from mid-April to mid-May but

withdraws abruptly in Pentads 3 – 5 in May, corresponding to the onset of the monsoon over the South China Sea. Afterwards; it extends west again and then goes back in Pentads 2 – 4 in June, corresponding to the time when the first northward jump of the subtropical high and the Mei-yu south of the Changjiang River are taking place. Then, the point begins its third advancement west and shrinks back east in Pentads 3 – 4 in July, corresponding to the second northward jump of the high. The westernmost ridge point tends to be stationary after the second jump.

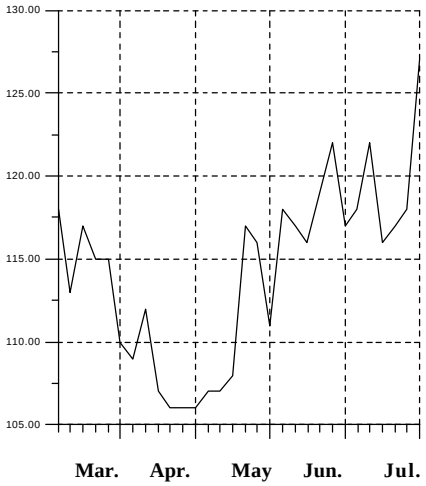

Fig.4 Pentad-to-pentad variation of the westernmost ridge point averaged over the 18 years.

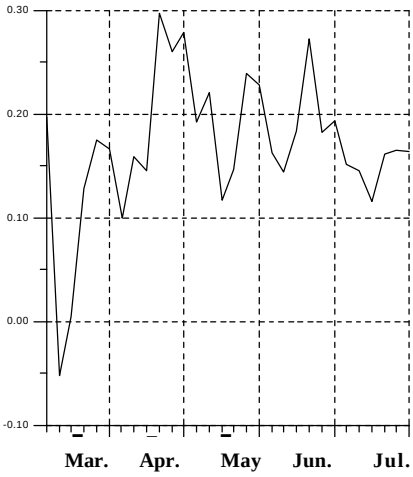

Fig.5 The first eigenvector of EOF analysis of the subtropical high westernmost ridge point.

3.3.3 VARIATION OF THE WESTERNMOST RIDGE POINT OF THE SUBTROPICAL HIGH DURING THE ONSET OF SOUTH CHINA SEA MONSOON IN LATE SPRING AND EARLY SUMMER

To study the behavior of the ridge point during the monsoon onset, we observe the yearly pattern of evolution. Our computation result indicates that the point tends to retreat east around the monsoon onset and usually starts to do so ahead of the monsoon establishment. It goes back for at least 7 degrees of longitude, except in 1994 (only four), with an average of 15 degrees. It is a sign that the ridge point changes drastically with the monsoon onset in the South China Sea.

3.4 *Variation of the ridge line of the subtropical high*

3.4.1 MEAN VARIATION TENDENCY FOR MARCH THROUGH JULY OVER THE 18 YEARS

For the study of the activity pattern of the subtropical high ridge line, more attention is placed on the two northward jumps of the ridge line during prime summer season than during the monsoon onset stage. Using the pentad-based 500-hPa geopotential height field in March through July in 1979 – 1996, mean variation of the ridge line has been determined over the 18 years, with reference to previous work in this aspect (Fig.6). It is clear that the pentad-to-pentad mean is generally consistent with what has been observed before, which reflects gradual northward movements of the ridge line with time and an obvious northward jump respectively in June and July. There are small north-south oscillations in all months of northward movement, which agrees with the result by Tang et al[5].

3.4.2 EOF ANALYSIS OF 18 YEARS

Like the intensity and westernmost ridge point, we apply a similar processing of the westernmost ridge point. It is done by giving an anomalous treatment of the data about the ridge line on the basis of pentad for March – July over the 18 years before the EOF analysis. It carries the physical idea It gives one the idea of several intraseasonal variations of the ridge point during the months and corresponding year-to-year changes.

As shown in the computation, the first eigenvector takes up about 25% of the total variance (table omitted). It can therefore represent the main features of the point's intraseasonal changes.

Fig.7 is about the first eigenvector, which describes the first pattern of intraseasonal variation. It is shown in the figure that the line gradually moves north in its north-south oscillation prior to mid-May but changes abruptly in Pentads 3 – 4 in May so as to retreat rapidly to the south, corresponding to the onset phase of the South China Sea monsoon. The line withdraws to the southernmost point in early June before an abrupt jump to the north in Pentads 1 – 2. It is the so-called first jump. Then, it makes alternative shifts until Pentads 2 – 3 in July when a second jump occurs and stabilizes. Graphically, such a pattern of variation looks like a robust reversed unimodal structure, i.e. drastic changes mainly occur at the point of monsoon onset and during the first northward jump.

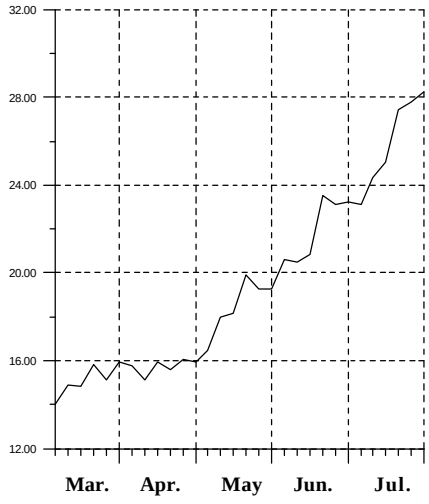

Fig.6 Pentad-to-pentad variation of the ridge line averaged over the 18 years.

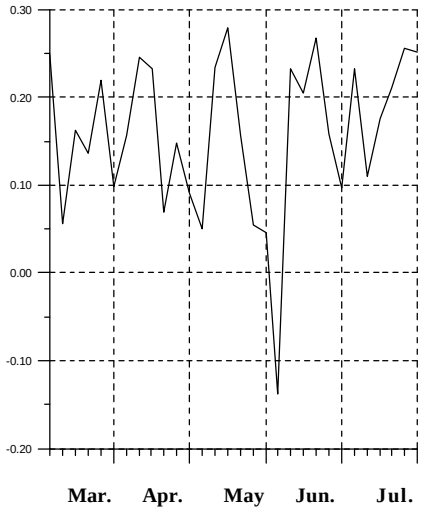

Fig.7 The first eigenvector of EOF analysis of the subtropical high ridge line.

4 INTERANNUAL VARIATION PATTERNS OF WESTERN PACIFIC SUBTROPICAL HIGH IN LATE SPRING AND EARLY SUMMER

In our definition of the subtropical high intensity, westernmost ridge point and ridge line, the values of the three on a pentad basis are added up for the period March through July each year to seek their relative mean and deviation from it. The three series are then processed with wavelet analysis, as in Fig.8a & b. It is now known that the interannual variation of the subtropical high intensity is significant of periodic oscillations around 4 and 8 years, with the former more pronounced. Furthermore, the oscillation is stronger in 1979 – 1992, suggesting that the intensity varies over a large amplitude over the time. The interannual variation is smaller in 1993 – 1996. Similarly, the interannual variation of the westernmost ridge point of the subtropical high is also of 4 and 8 years in period, with the former more obvious. The more significant variation is also seen in 1972 – 1992. The interannual variation of the ridge line is only of four years while the

more pronounced variation is found in the years 1979 – 1992.

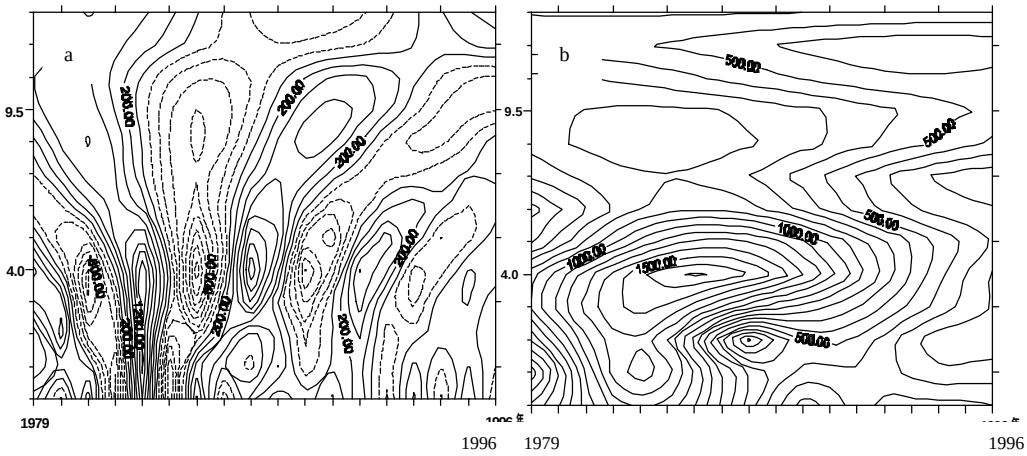

Fig.8 The real part of the wavelet transform analysis in the interannual variation of the subtropical high (a) and coefficient module of the contours (b). The ordinate is for the year of corresponding periods.

5 CONCLUDING REMARKS

With the NCEP/NCAR dataset of the 500-hPa geopotential height field for March through July in 1979 – 1996, the current work applies anomaly approach, wavelet transform and EOF analysis to the intensity, westernmost ridge point and ridge line of the subtropical high in the western Pacific and yields results of the evolution of the high in late spring and early summer. The following are the main conclusions:

a. As the time passes from March to July, the subtropical high intensifies. There are, however, three abrupt changes in the intraseasonal variation. The first happens in Pentads 3 – 5 in May when the high suddenly weakens; the second in Pentads 2 – 3 in June when it suddenly intensifies; the third in Pentads 3 – 5 in July when it strengthens again.

b. The westernmost ridge point gradually extends westward from March to July, reaching its most western location around the end of April and early May before a sudden retreat to the east in Pentads 3 – 4 in May (over an average distance of about 15 longitudes). Afterwards, the point oscillates alternatively in a generally eastward progression. Like the case of intensity, the point also has three abrupt changes in the intraseasonal variation, first being in Pentads 3 – 5 in May when it withdraws suddenly to the east, the second in Pentads 2 – 4 in June when it replays the withdrawal; the third in Pentads 3 – 4 in July when it goes back eastward for the third time.

c. The ridge line of the subtropical high moves slowly north with time over the months March – July, though with an obvious northward jump in mid-June and mid-July. Like the cases of intensity and westernmost ridge point, the line also experiences three times of abrupt change in the intraseasonal variation, first being in Pentads 3 – 5 in May when it withdraws suddenly to the south, the second in Pentads 1 – 2 in June when it suddenly jumps north; the third in Pentads 2 – 4 in July when it goes back southward for the second time.

d. For the three abrupt changes in the intraseasonal variation of the subtropical high in March – July, there are correspondingly the onset of the South China Sea monsoon, the first and second northward jumps on the synoptic scale. Before the onset of the monsoon in mid-May, the subtropical high abruptly weakens, the westernmost ridge point retreats eastward and the ridge line goes back to the south. During the Mei-yu period south of the Changjiang R.basin in

mid-June, the subtropical high suddenly intensifies, the point withdraws to the east and the line jumps to the north. When the subtropical high strengthens again, the westernmost ridge point withdraws eastward and the ridge line jumps northward for the second time in mid-July, the Mei-yu ends and a raining season begins in northern China.

e. The intensity, the westernmost ridge point and the ridge line all have periods at around 4 and 8 years in the interannual variation, though being insignificant with the line for the 8-year period. The 4-year period is more pronounced, with the period of strongest oscillation concentrating in the years 1979 – 1992, followed by one of the relative weak oscillations after 1992.

Acknowledgements: Mr. CAO Chao-xiong, who works at the Institute of Tropical and Marine Meteorology, CMA, Guangzhou, has translated the paper into English..

REFERENCES:

[1] ZHANG Qing-yun, TAO Shi-yan. A study on the northward jumps of subtropical high in the western Pacific in summertime and its anomalies [J]. *Acta Meteorologica Sinica*, 1997, **10**: 539-547.
[2] HUANG Shi-song. A study on the activity of subtropical high and the forecasting [J]. *Chinese Journal of Atmospheric Sciences*, 1978, **6**: 159-167.
[3] MADDEN R D**,** JULIAN P. Detection of a 40-50 day oscillation in the zonal wind in the tropical Pacific [J]. *Journal of Atmospheric Science*, 1971, **28**: 702-708.
[4] KRISHNAMURI T N, SUBRAHMANYAM D. The 30-50 day mode at 850 hPa during MONEX [J]. *Journal of Atmospheric Sciences*, 1982, **39**: 2088-2095.
[5] TANG Ming-min, LU Seng-e, HUAGN Shi-song. On the variation of the subtropical high location in the western Pacific [A]. Collection of Papers on Tropical Circulation and Systems [C]. Beijing: Ocean Press, 1982. 153-167.
[6] ZHAO Zhen-guo, CHEN Guo-zhen. Characteristics of the location and intensity of the western Pacific subtropical high [J]. *Journal of Tropical Meteorology*, 1995, **8**: 223-230.
[7] HUANG Jia-you. Statistical Analysis and Forecasting Techniques in Meteorology [M]. Beijing: Meteorological Press, 1990. 170-197.
[8] SHI Neng. Multivariate Analysis Methods in Meteorological Research and Forecasting [M]. Beijing: Meteorological Press, 1995. 134-200.
[9] DENG Ai-jun, TAO Shi-yan, CHEN Lie-ting. EOF analysis of precipitation in the raining season of China [J]. *Chinese Journal of Atmospheric Sciences*, 1989, **9**: 289-295.
[10] XIE Li. Wavelet analysis of the 1000-hPa geopotential height field in the South China Sea [J]. *Journal of Zhongshan Univeristy Postgraduates* (*edition of natural science*), 1999, (1): 21-26.
[11] CUI Jin-tai. An Introduction to Wavelet Analysis [M]. Xi'an: Xi'an Communications University Press, 1995. **17**: 58-72.
[12] HU Zeng-zhen, SHI Wei. The application of sub-waves transform in the atmospheric science [J]. *Chinese Journal of Atmospheric Sciences*, 1997, **17**: 58-72.
[13] LIU Xia, XIE An, YE Qian, et al. Climatological features of the summer monsoon onset in the South China Sea [J]. *Journal of Tropical Meteorology*, 1998, **14**: 28-37.
[14] WANG Li-juan, HE Ji-hai, XU Hai-ming, et al. Abrupt changes around the onset of South China Sea summer monsoon in 1998 and the outbreak process [J]. *Journal of Nanjing Institute of Meteorology*, 1999, **6**: 136-140.
[15] TSUYUKI T, KURIHARA K. On the role convective activity in the western tropical Pacific in the formation of the barotropic high around Japan during summer[J]. *Tropical rainfall measurement*,1988(**1**): 93-99.
[16] LUO Jing-jia, HE Jing-hai. The patterns of summer monsoon establishment in Asia and South China Sea onset characteristics and a preliminary study on the causes [J]. *Journal of Nanjing Institute of Meteorology*, 1997, **9**: 293-300.
[17] CHEN Long-xun, LIU Hong-qing, WANG Wen et al. A preliminary study of the summer monsoon onset in the South China Sea and the adjacent regions and its mechanisms [J]. *Acta Meteorologica Sinica*, 1999, **52**: 16-19.
[18] KASAHARA A, BALGOVIND R C, KATZ B B. Use of satellite radiometric imagery data for improvement in the analysis of divergent wind in tropics [J]. *Monthly Weather Review*, 1988, **116**: 866-883.